

## Article

# Influence of Power Supply Ripple on Injection Locking of Magnetron with Frequency Pushing Effect

Zihao Zhang, Yongjie Zhou, Shimiao Lai, Ge Wang, Huacheng Zhu  and Yang Yang \*

College of Electronics and Information Engineering, Sichuan University, Chengdu 610065, China

\* Correspondence: yyang@scu.edu.cn

**Abstract:** The influence of anode voltage ripple on injection locking of a magnetron with frequency pushing effect has been studied systematically. Theoretical analysis shows that, when power supply ripple and injection ratio are constant, frequency pushing effect will increase the magnetron's locking bandwidth. Meanwhile, the locking bandwidth decreases with the increase of power supply ripple. Thus, to achieve injection locking, both power supply ripple and frequency pushing effect must be considered. The experiment results show that at injection ratio  $\mu$  of 0.003, frequency pushing effect at 0.5, and power supply ripple increases from 0% to 1% and 2.5%, the locking bandwidth of magnetron decreases by 0.32 MHz, 2.12 MHz. With the amplitude of ripple increasing, the spectrum after injection locking deteriorates, and output amplitude reduces, which verifies the theoretical analysis. Considering anode voltage ripple and frequency pushing effect, the research results contribute to the realization of high-quality output of injection locked magnetrons.

**Keywords:** power supply ripple; magnetron; injection locking; frequency pushing effect



**Citation:** Zhang, Z.; Zhou, Y.; Lai, S.; Wang, G.; Zhu, H.; Yang, Y. Influence of Power Supply Ripple on Injection Locking of Magnetron with Frequency Pushing Effect. *Processes* **2022**, *10*, 2124. <https://doi.org/10.3390/pr10102124>

Academic Editors: Alon Kuperman and Alessandro Lampasi

Received: 25 September 2022

Accepted: 17 October 2022

Published: 19 October 2022

**Publisher's Note:** MDPI stays neutral with regard to jurisdictional claims in published maps and institutional affiliations.



**Copyright:** © 2022 by the authors. Licensee MDPI, Basel, Switzerland. This article is an open access article distributed under the terms and conditions of the Creative Commons Attribution (CC BY) license (<https://creativecommons.org/licenses/by/4.0/>).

## 1. Introduction

The magnetron is an important and widely-used high-power microwave device [1], with merits of high-efficiency output power, low cost and low weight [2,3], on which microwave heating [4,5], microwave communication jamming [6], and microwave wireless power transferring [7,8] rely. However, the output of free oscillating magnetrons has a lot of deficiencies, including the scattered output power, the erratic output frequency and the instable spectrum, which restrict the applications of magnetrons.

In order to improve the efficiency of magnetrons, great efforts have been made by researchers. Adler [9] proposed the theory of injection locking, which locks the output frequency with a low-power reference signal injected to the magnetron. Mitani [10] demonstrated turning off the filament current to improve the output when the filament works well with reshock electrons. Moreover, the relationship between the power supply ripple and the locking bandwidth was reported innovatively by Chen et al. [11]. Meanwhile Zhou et al. [12] analyzed the influence of anode voltage on the output power and frequency. S. C. Chen [13] and Li. et al. [14] extended the traditional Adler Equation [9] by considering the frequency pushing effect theoretically and experimentally.

However, with the further expansion of applications, the output stability of magnetrons is further demanded. For microwave plasma chemical vapor deposition (MPCVD) [15], microwave medical treatment [16,17], and other microwave chemistry industrials [18], which are very sensitive to the frequency and the performance of power supply, the improvements precious can no longer meet the requirements.

So, the influence of anode voltage ripple on injection locking of magnetron with frequency pushing effect is proposed innovatively in this paper, which provides the theoretical guidance for the higher quality of spectra. The relationship between output amplitude and locking frequency has been proposed theoretically under different power supply ripples, injection ratios and frequency pushing effects. The numerical simulation analysis shows

that, with constant injection ratio and frequency pushing effect, when the power ripple increases, the locking bandwidth and the output amplitude decrease. As for the injection frequency, when it is equal to the free-oscillating frequency without frequency pushing effect, the output amplitude reaches the largest. However, when it is slightly different from the free-oscillating frequency, the output amplitude is the largest, concerning the frequency pushing effect. Furthermore, the increase of ripples does not affect the injection frequency with the largest output amplitude. Finally, an experiment is set up to testify the theoretical derivation.

## 2. Theory and Analysis

### 2.1. Theoretical Analysis of Injection Locking with Ripple and Frequency Push Effect

According to Slater’s theory [19], a single-mode operating (usually  $\pi$ -mode) magnetron can be equivalent to a parallel resonant circuit composed of lumped components, as shown in Figure 1, the electron admittance is represented by  $(g + jb)$ ; the magnetron resonance cavity is approximated by a resistor–inductor–capacitor (RLC) resonant circuit; and the external load is then regarded as the load admittance  $(G + jB)$ . However, magnetron is one of the vacuum tubes with complex frequency shift effect, and the equivalent circuit equations with frequency push effect  $\alpha$  are as follows:

$$\frac{g + jb}{C\omega_0} = i\left(\frac{\omega}{\omega_0} - \frac{\omega_0}{\omega}\right) + \frac{1}{Q_0} + \frac{G + jB}{Q_{ext}} \tag{1}$$

$$b = b_0 - g \tan \alpha \tag{2}$$

$$g = \frac{1}{R} \left(\frac{V_{dc}}{V_{RF}} - 1\right) \tag{3}$$

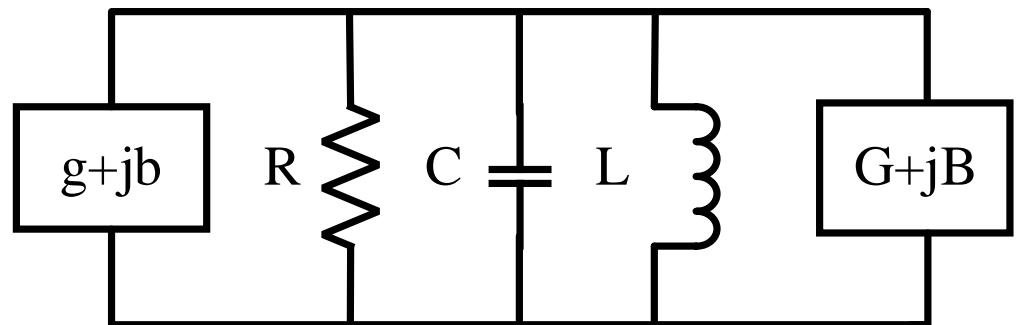


Figure 1. Equivalent circuit of magnetron.

$b_0$  and  $\alpha$  are constants defined by the magnetron itself.  $\omega$  is the magnetron’s output frequency,  $\omega_0$  is the resonance frequency, and  $Q_0$  and  $Q_{ext}$  are the unloaded and external loaded quality factors.  $V_{dc}$  and  $V_{RF}$  are anode voltage and radio frequency (RF) output of the magnetron.

The reference signal with the frequency  $\omega'$ , the phase difference  $\theta$  is injected into a magnetron. Injection ratio  $\rho$  is the ratio of injection intensity to magnetron output intensity. The amplitude of RF voltage and the first derivative of phase with time can be represented by the following equation [19]:

$$V_{RF} = \frac{V_{RF0}}{1 + \frac{\mu \cos \theta}{\frac{\omega_0}{2} \left(\frac{1}{Q_L} + \frac{1}{RC\omega_0}\right)}} \tag{4}$$

$$\frac{d\theta}{dt} = \frac{\rho \omega_0}{Q_{ext} |\cos \alpha|} \sin(\theta - \alpha) + \frac{\omega' - \omega}{\omega_0} \tag{5}$$

$$\frac{1}{Q_L} = \frac{1}{Q_0} + \frac{G}{Q_{ext}} \tag{6}$$

where  $V_{RF0}$  is the output amplitude of free-oscillating magnetron,  $Q_L$  represents the loaded quality factor and  $\omega$  is equal to the frequency of the injected signal.  $\mu = \rho / Q_{ext}$  represents the injection amplitude. When the injection locking is achieved, the phase difference  $\theta$  is a constant and  $d\theta/dt$  equals to zero in Equation (5). So, the following equation can be derived:

$$\theta = \arcsin\left(\frac{\omega' - \omega}{\omega_0} \frac{|\cos\alpha|}{\mu}\right) \tag{7}$$

Introducing Equation (7) into Equation (4) [14], Equation (8) is obtained.

$$V_{RF} = \frac{V_{RF0}}{1 + \frac{2\mu}{\omega_0(\frac{1}{Q_L} + \frac{1}{RC\omega_0})} \cos(\arcsin\left(\frac{\omega - \omega'}{\omega_0} \frac{|\cos\alpha|}{\mu}\right) + \alpha)} \tag{8}$$

The anode voltage of the magnetron is supplied by high power supply. Because there is no perfect rectification, anode voltage will have a certain ripple. Therefore, the high voltage power supply  $V'_{dc}$  can be regarded as two parts: one is the high voltage  $V_{dc}$  of DC power supply, and the other is the slowly varying ripple. Root mean square (RMS) voltage can express the anode voltage with slow-changing fluctuation [11]. So, the anode voltage can be expressed as follows:

$$V'_{dc} = V_{dc} \left(1 + \frac{S}{2\sqrt{2}}\right) \tag{9}$$

where  $S = V_{p-p} / V_{dc}$  is the ripple parameters,  $V_{p-p}$  is peak to peak of ripple. Introducing Equation (9) into Equation (8), Equation (10) is obtained.

$$\frac{V_{RF}}{V_{RF0}} = \frac{\left(1 + \frac{S}{2\sqrt{2}}\right)}{1 + \frac{2\mu}{\omega_0(\frac{1}{Q_L} + \frac{1}{RC\omega_0})} \cos(\arcsin\left(\frac{\omega - \omega'}{\omega_0} \frac{|\cos\alpha|}{\mu}\right) + \alpha)} \tag{10}$$

Equation (10) describes the relationship between the output amplitude and the frequency of the injection locked magnetron under the influence of power supply ripple  $S$ , frequency push effect  $\alpha$  and injection amplitude  $\mu$ .

### 2.2. Numerical Simulation of Injection Locking with Ripple and Frequency Push Effect

Based on Equation (10), a numerical analysis is carried out to prove the relative output amplitude with respect to the normalized frequency of the injection locked magnetron under various parameters as shown in in Figure 2.

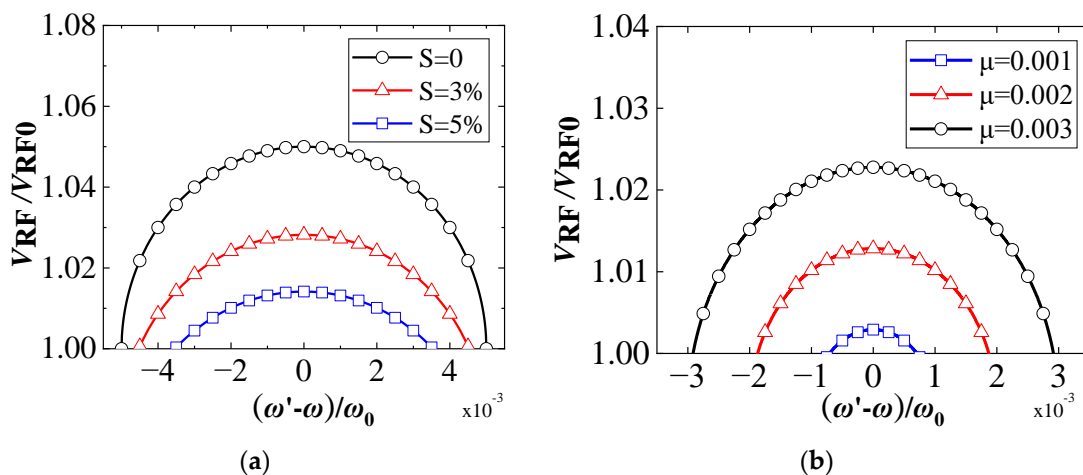


**Figure 2.** The injection locking performance with respect to the (a) power supply ripple  $S$  and (b) injection amplitude  $\mu$ , without the frequency pushing effect  $\alpha$ .

The relative amplitude is  $V_{RF}/V_{RF0}$ , and the locking bandwidth and injection frequency is the normalized frequency difference given by  $(\omega' - \omega)/\omega_0$ .

When injection amplitude  $\mu$  is 0.005 and frequency push effect  $\alpha$  is 0, each curve is plotted with respect to power supply ripple in Figure 2a. The detailed data of injection locking under different ripple are shown in Table 1. In the case of frequency push effect  $\alpha = 0$  and injection amplitude  $\mu = 0.005$ , when the ripple  $S$  increases from 0 to 3% and 5%, locking bandwidth decreases from  $5.00 \times 10^{-3}$  to  $4.53 \times 10^{-3}$  and  $3.5 \times 10^{-3}$ . The output amplitude reaches the maximum, when there is no difference between the injection frequency and free-oscillating frequency. When the amplitude of ripple increases, the maximum output decreases from 1.050 to 1.014. If the ripple continues to increase, the locking bandwidth turns 0 and the locking status cannot be realized.

**Table 1.** Comparison of injection locking in different ripples.

Ripples $S$	0%	3%	5%
Locking bandwidth	$5.00 \times 10^{-3}$	$4.53 \times 10^{-3}$	$3.5 \times 10^{-3}$
Injection frequency with largest output amplitude	0	0	0
Largest output amplitude	1.050	1.028	1.014

When the ripples  $S$  is 1% and frequency push effect  $\alpha$  is 0, Figure 2b displays the relative output amplitude with respect to injection amplitude. The detailed data of injection locking under different injection amplitude are shown in Table 2. In the case of the ripple  $S = 1\%$  and frequency push effect  $\alpha = 0$ , when injection amplitude  $\mu$  increases from 0.001 to 0.002 and 0.003, the locking bandwidth increases from  $0.68 \times 10^{-3}$  to  $1.85 \times 10^{-3}$  and  $2.9 \times 10^{-3}$ . The output amplitude reaches the maximum, when there is no difference between the injection frequency and free-oscillating frequency. With the increase of injection amplitude, the maximum output increases from 1.003 to 1.023. Because of ripple  $S$ , the locking bandwidth of the three curves is slightly lower than the injection amplitude.

**Table 2.** Comparison of injection locking in different injection amplitude.

Injection Amplitude $\mu$	0.001	0.002	0.003
Locking bandwidth	$0.68 \times 10^{-3}$	$1.85 \times 10^{-3}$	$2.90 \times 10^{-3}$
Injection frequency with largest output amplitude	0	0	0
Largest output amplitude	1.003	1.013	1.023

The amplitude is  $V_{RF}/V_{RF0}$ , and the locking bandwidth and Injection frequency is the normalized frequency difference given by  $(\omega' - \omega)/\omega_0$ .

In Figure 3, the stability conditions and locking bandwidth are affected by the frequency push effect  $\alpha$ . When  $\alpha$  increases, the locking bandwidth of magnetron also increases, and the stable region becomes larger.

From Figure 3a, in the case of frequency push effect  $\alpha = 0.5$  and injection amplitude  $\mu = 0.002$ , when the ripple  $S$  increases from 0 to 1% and 2%, the locking bandwidth and the output energy decreases. The detailed data of injection locking under different ripples are shown in Table 3. When the amplitude of ripples increases, the locking bandwidth diminishes from  $2.28 \times 10^{-3}$  to  $1.35 \times 10^{-3}$  and largest output amplitude decreases from 1.020 to 1.006. Due to frequency push effect  $\alpha$ , the output amplitude cannot reach the maximum value, at the time of free-oscillating frequency equaling to the injection one. However, the increase of ripple does not affect the injection frequency with the largest output amplitude, which is always  $1.09 \times 10^{-3}$ .

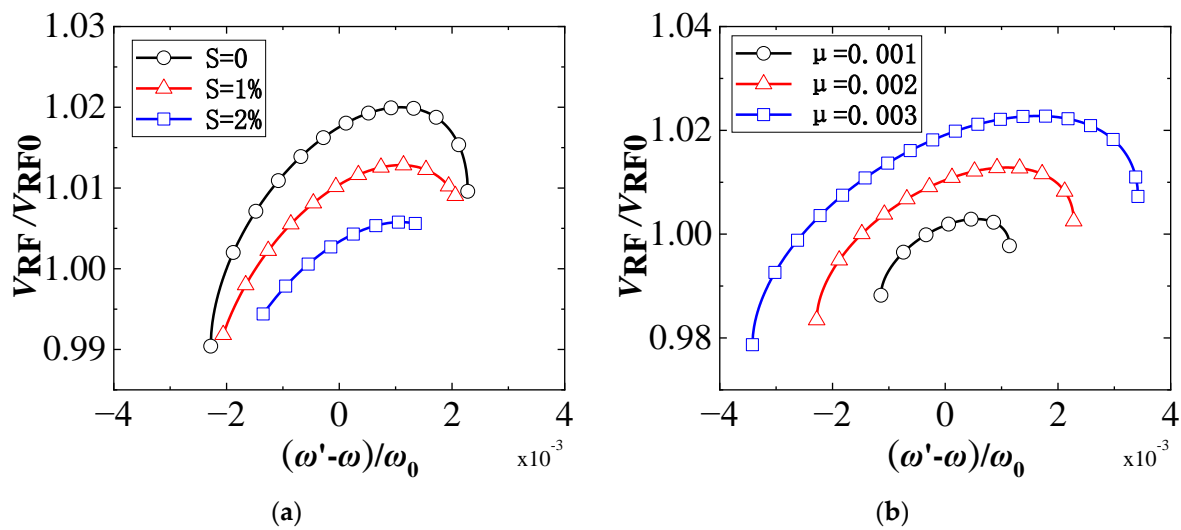


**Figure 3.** The injection locking performance with respect to the (a) power supply ripple  $S$  and (b) injection amplitude  $\mu$ , with the frequency pushing effect  $\alpha$ .

**Table 3.** Comparison of injection locking in different ripples.

Ripples $S$	0%	1%	2%
Locking bandwidth	$2.28 \times 10^{-3}$	$2.06 \times 10^{-3}$	$1.35 \times 10^{-3}$
Injection frequency with largest output amplitude	$1.09 \times 10^{-3}$	$1.09 \times 10^{-3}$	$1.09 \times 10^{-3}$
Largest output amplitude	1.020	1.013	1.006

In Figure 3b, in the case of frequency push effect  $\alpha = 0.5$  and the ripple  $S = 1\%$ , when injection amplitude  $\mu$  increases from 0.001 to 0.002 and 0.003, the locking bandwidth and the output energy increases. The detailed data of injection locking under different injection amplitude are shown in Table 4. With the increase of injection amplitude, the maximum output increases from 1.003 to 1.023. Due to frequency push effect  $\alpha$ , the output amplitude cannot reach the maximum value, at the time of free-oscillating frequency equaling to the injection one. However, with the increase of injection amplitude  $\mu$ , the injection frequency with the maximum output amplitude increases from  $0.55 \times 10^{-3}$  to  $1.64 \times 10^{-3}$ .

**Table 4.** Comparison of injection locking in different injection amplitude.

Injection Amplitude $\mu$	0.001	0.002	0.003
Locking bandwidth	$1.14 \times 10^{-3}$	$2.08 \times 10^{-3}$	$3.42 \times 10^{-3}$
Injection frequency with largest output amplitude	$0.55 \times 10^{-3}$	$1.09 \times 10^{-3}$	$1.64 \times 10^{-3}$
Largest output amplitude	1.003	1.013	1.023

### 3. Experimental Setup

Based on the schematic diagram (Figure 4a), the experimental system was set to verify the theoretical analysis (Figure 4b). The microwave power which is generated by the magnetron (2M244-M1, Panasonic, Osaka, Japan) is transferred from Port #1 to Port #2 of the three-port circulator, and partial energy is coupled by the double directional coupler to visualize using power meter and real-time signal analyzer. Moreover, the spare microwave power from Port #2 and form Port #2 to Port #3 is absorbed by the water load. A solid-state source is used for energy source of injection locking. Through the circulator, the energy of the solid-state source is injected into the magnetron. A small part of the locked signal is coupled by a coupler. Then its spectrum and energy are measured by a power meter and signal analyzer. The power supply ripple of magnetron is reduced by paralleling filtering

capacitor and measured by oscilloscope. The energy of the whole system is absorbed by the water loads.

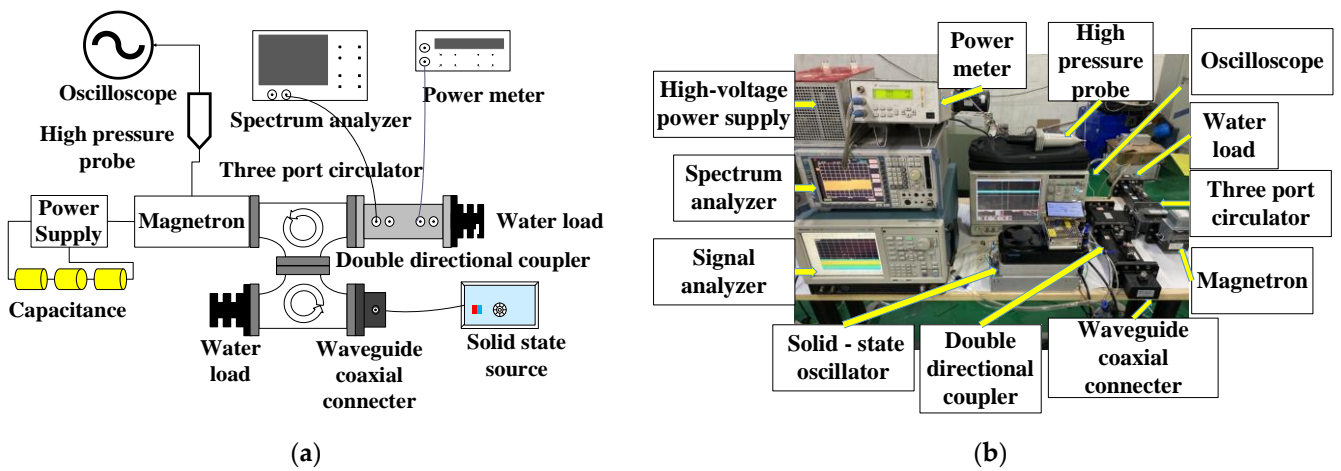


Figure 4. (a) Experimental schematic diagram, and (b) Photograph of the experimental system.

#### 4. Results and Discussions

The measured relative output amplitude with respect to normalized frequency of injection locked magnetron is shown in Figure 5. Under the condition of the frequency pushing effect  $\alpha = 0.5$  and injection amplitude  $\mu = 0.003$ , if the ripple  $S$  grows from 0 to 1% and 2.5%, the measured locking bandwidth and the measured output energy decreases, which are basically corresponding to the theoretical values with the same varying tendency.

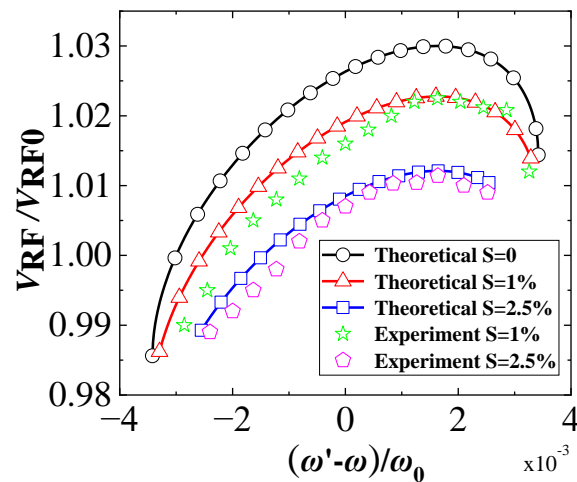


Figure 5. Experimental and theoretical injection locking performance with respect to the power supply ripple  $S$ .

Locked bandwidth is  $\omega' - \omega$  in MHz. Injection frequency is the normalized frequency difference given by  $(\omega' - \omega)/\omega_0$  and the amplitude is  $V_{RF}/V_{RF0}$ .

The detailed data of theoretical and measured locking bandwidths under different ripple are shown in Table 5. When the ripples  $S$  are 0, 1%, 2.5% respectively, ignoring frequency push effect, theoretical locking bandwidths are 7.35 MHz, 7.15 MHz and 5.93 MHz respectively. However, while the frequency pushing effect  $\alpha$  is set to 0.5, theoretical locking bandwidths are 8.38 MHz, 8.06 MHz and 6.26 MHz, respectively. Furthermore, the measured locking bandwidths are 7.99 MHz and 6.19 MHz, which are only 0.07 MHz and 0.09 MHz different from the theoretical value, respectively. When the normalized injection frequency is  $1.64 \times 10^{-3}$ , which is slightly different from the free oscillation frequency, the output amplitude reaches the maximum. Measured largest output amplitude is 1.022

and 1.011 with the increasing of ripples, which is only 0.001 different from the theoretical value. Above experimental data are consistent with the theory. It is worth noting that the measured curve is asymmetrical, instead of the symmetrical one about the free oscillating frequency, which was derived in reported issues, such as [11]. And it is the evidence of the influence of the frequency pushing effect on the locking performance considering the power supply ripple.

**Table 5.** Theoretical and experimental bandwidth locking under different ripple and pushing effect.

Ripples $S$	0%	1%	2.5%
Theoretical locked bandwidth in $\alpha = 0$	7.35	7.15	5.93
Theoretical locked bandwidth in $\alpha = 0.5$	8.38	8.06	6.26
Measured locked bandwidth in $\alpha = 0.5$		7.99	6.17
Theoretical injection frequency with largest output amplitude in $\alpha = 0.5$	$1.64 \times 10^{-3}$	$1.64 \times 10^{-3}$	$1.64 \times 10^{-3}$
Theoretical Largest output amplitude in $\alpha = 0.5$	1.030	1.023	1.012
Measured injection frequency with largest output amplitude in $\alpha = 0.5$		$1.64 \times 10^{-3}$	$1.64 \times 10^{-3}$
Measured Largest output amplitude in $\alpha = 0.5$		1.022	1.011

Then, the injection amplitude  $\mu$  is changed to 0.001, 0.002 and 0.003, while the power supply ripple  $S$  is maintained at 2.5%. Moreover, the output spectra of the magnetron are shown in Figure 6a–c, respectively. When the ripple  $S = 1\%$  and the injection amplitude is 0.001, 0.002 and 0.003 respectively, the DPX output spectra of the magnetron are shown in Figure 7a–c, respectively. The DPX spectrum can keep up with the fast change speed to display more vivid output parameters. And the brighter the color, the more frequently the frequency points appear.

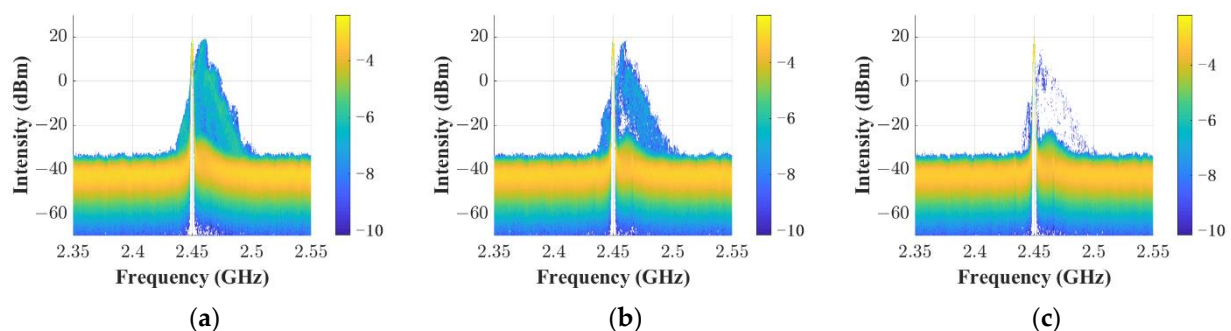


**Figure 6.** Measured DPX spectra of the magnetron with injecting amplitude at (a) 0.001, (b) 0.002 and (c) 0.003 under the power supply ripple  $S = 2.5\%$ .

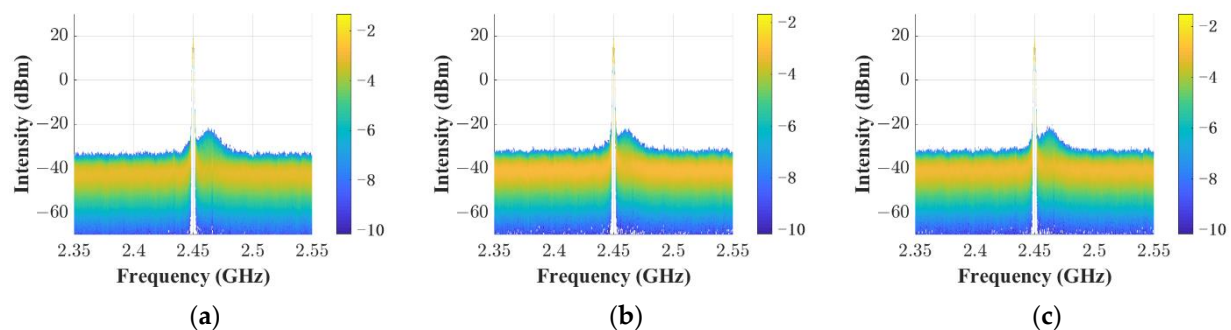


**Figure 7.** Measured DPX spectra of the magnetron with injecting amplitude at (a) 0.001, (b) 0.002 and (c) 0.003 under the power supply ripple  $S = 1\%$ .

In Figure 6, when the ripple  $S = 2.5\%$ , the magnetron is locked gradually with the increase of injection amplitude  $\mu$ . When the injection amplitude is 0.001 and 0.002, the magnetron is still unlocked, and the output spectrum is full of noise jitter. When the

injection amplitude is 0.003, the magnetron is locked, and the spectrum has been greatly improved. In Figure 7, with the decreased ripple, when the injection amplitude  $\mu$  is only 0.001, the magnetron can be locked, and a high-quality spectrum can be output. Through the DPX spectrum, we verify that when the ripple is smaller, it is easier to achieve injection locking and pure spectrum.

## 5. Conclusions

The performance of injection-locked magnetron is jointly impacted by the power supply ripple and the frequency pushing effect. In this paper, firstly, the equivalent circuit was adopted to obtain the expression of the locking bandwidth with respect to the power supply ripple  $S$  and the frequency pushing effect  $\alpha$ , and the locking performance was obtained by the numerical simulation, which was an asymmetrical curve, different from the curve derived by the traditional Adler equation. With the increasing of the power supply ripple  $S$ , the locking bandwidth was reducing. Conversely, it was getting wider when the injection amplitude  $\mu$  increased. Then, the experiments were set up to verify the theoretical derivation. The reduction of the power supply ripple was achieved through a paralleling filtering capacitor. The measured relative amplitude curve with respect to a different ripple  $S$  was in good agreement with the simulation. The actual results of the locking bandwidth were consistent with the simulation one with the frequency pushing effect basically, which meant that the parameter  $\alpha$  indeed affected the locking performance. In addition, we found that the injection frequency corresponding to the max output amplitude was slightly different from the free oscillating frequency, due to the frequency pushing effect.

Compared with the reported issues, we extend the theory of the influence of the power supply ripple on the injection-locking performance by the frequency pushing effect. This research promises to be applied to microwave plasma and chemistry industrials for highly stable magnetrons.

**Author Contributions:** Z.Z. developed the model, finished the experiment, analyzed the data, and wrote the initial draft of the manuscript; Y.Z., S.L. and G.W. conceived and designed the experiment; H.Z. and Y.Y. reviewed and contributed to the final manuscript. All authors have read and agreed to the published version of the manuscript.

**Funding:** This research was funded by the Sichuan Science and Technology Program under grant 2021YFG0265 and Key Technology of Shunde District under Grant 2130218002514.

**Data Availability Statement:** Not applicable.

**Conflicts of Interest:** The authors declare no conflict of interest.

## References

1. Gilmour, A.S. *Klystrons, Traveling Wave Tubes, Magnetrons, Crossed-field Amplifiers, and Gyrotrons*; Artech House: Norwood, MA, USA, 2011.
2. Chen, C.; Huang, K.; Yang, Y. Microwave transmitting system based on four-way master–slave injection-locked magnetrons and horn arrays with suppressed sidelobes. *IEEE Trans. Microw. Theory Tech.* **2018**, *66*, 2416–2424.
3. Booske, J.H. Plasma physics and related challenges of millimeterwave-to-terahertz and high-power microwave generation. *Phys. Plasmas* **2008**, *15*, 459–597. [[CrossRef](#)]
4. Yang, Y.; Fan, Z.; Hong, T.; Chen, M.; Tang, X.; He, J.; Chen, X.; Liu, C.; Zhu, H.; Huang, K. Design of Microwave Directional Heating System Based on Phased-Array Antenna. *IEEE Trans. Microw. Theory Tech.* **2020**, *68*, 4896–4904. [[CrossRef](#)]
5. Zhang, W.; Tao, J.; Huang, K.; Wu, L. Numerical Investigation of the Surface Wave Formation in a Microwave Plasma Torch. *IEEE Trans. Plasma Sci.* **2017**, *45*, 2929–2939. [[CrossRef](#)]
6. Yang, Y.; Li, K.; Li, J.; Zhu, H.; Zhang, Y.; Huang, K. Low-Cost, High-Power Jamming Transmitter Based on Magnetron. *IEEE Trans. Electron Devices* **2020**, *67*, 2912–2918. [[CrossRef](#)]
7. Brown, W. The History of Power Transmission by Radio Waves. *IEEE Trans. Microw. Theory Tech.* **1984**, *32*, 1230–1242. [[CrossRef](#)]
8. Shinohara, N. Beam Control Technologies with a High-Efficiency Phased Array for Microwave Power Transmission in Japan. *Proc. IEEE* **2013**, *101*, 1448–1463. [[CrossRef](#)]
9. Adler, R. A study of locking phenomena in oscillators. *Proc. Inst. Radio Eng.* **1946**, *34*, 351–357. [[CrossRef](#)]

10. Mitani, T.; Shinohara, N.; Matsumoto, H.; Aiga, M.; Kuwahara, N. Experimental research on noise reduction of magnetrons for solar power station/satellite. In Proceedings of the 2004 Asia-Pacific Radio Science Conference, Qingdao, China, 24–27 August 2005. [[CrossRef](#)]
11. Chen, X.; Yu, Z.; Lin, H.; Zhao, X.; Liu, C. Improvements in a 20-kW Phase-Locked Magnetron by Anode Voltage Ripple Suppression. *IEEE Trans. Plasma Sci.* **2019**, *48*, 1879–1885. [[CrossRef](#)]
12. Zhou, Y.; Zhang, Y.; Zhu, H.; Yang, Y. Study of the Influence of Power Supply Ripple on Magnetron's Output Spectrum. *IEEE Trans. Electron Devices* **2021**, *68*, 4698–4704. [[CrossRef](#)]
13. Chen, S.C. Growth and frequency pushing effects in relativistic magnetron phase-locking. *IEEE Trans. Plasma Sci.* **1990**, *18*, 570–576. [[CrossRef](#)]
14. Li, K.; Zhang, Y.; Zhu, H.; Huang, K.; Yang, Y. Theoretical and experimental study on frequency pushing effect of magnetron. *Chinese Physics B* **2019**, *11*, 431–436.
15. Su, J.; Li, Y.; Ding, M.; Tang, W. Development of cylindrical cavity type microwave plasma chemical vapor deposition reactor for diamond films deposition. In Proceedings of the Abstracts IEEE International Conference on Plasma Science (ICOPS), San Francisco, CA, USA, 16–21 June 2013; p. 1. [[CrossRef](#)]
16. Chandra, R.; Zhou, H.; Balasingham, I.; Narayanan, R.M. On the Opportunities and Challenges in Microwave Medical Sensing and Imaging. *IEEE Trans. Biomed. Eng.* **2015**, *62*, 1667–1682. [[CrossRef](#)] [[PubMed](#)]
17. Wang, W.; Mandelis, A. Microwave-heating-coupled photoacoustic radar for tissue diagnostic imaging. *J. Biomed. Opt.* **2016**, *21*, 066018. [[CrossRef](#)] [[PubMed](#)]
18. Huang, K.; Zhou, Y.; Wu, L. Research on Microwave Chemistry in Sichuan University. In Proceedings of the 2018 Asia-Pacific Microwave Conference (APMC), Kyoto, Japan, 6–9 November 2018. [[CrossRef](#)]
19. Slater, J.C. The phasing of magnetrons. In *Research Laboratory of Electronics*; MIT: Cambridge, MA, USA, 1947; Volume 35.